



## An ISFET biosensor for the monitoring of maltose-induced conformational changes in MBP

Hye-Jung Park<sup>a</sup>, Sang Kyu Kim<sup>a,b</sup>, Kyoungsook Park<sup>a</sup>, Hong-Kun Lyu<sup>c</sup>, Chang-Soo Lee<sup>a</sup>, Sang J. Chung<sup>a</sup>, Wan Soo Yun<sup>d</sup>, Moonil Kim<sup>a,b,\*</sup>, Bong Hyun Chung<sup>a,b,\*</sup>

<sup>a</sup>BioNanotechnology Research Center, Korea Research Institute of Bioscience and Biotechnology (KRIBB), Daejeon 305-333, South Korea

<sup>b</sup>School of Engineering, University of Science and Technology (UST), Daejeon 305-333, South Korea

<sup>c</sup>Daegu Gyeongbuk Institute of Science and Technology, Daegu 704-230, South Korea

<sup>d</sup>Korea Research Institute of Standards and Science (KRISS), Daejeon 305-600, South Korea

### ARTICLE INFO

#### Article history:

Received 20 October 2008

Revised 19 November 2008

Accepted 21 November 2008

Available online 6 December 2008

Edited by Miguel De la Rosa

#### Keywords:

ISFET

Biosensor

Surface charge

Conformational change

MBP

### ABSTRACT

**Here we describe an ion sensitive field effect transistor (ISFET) biosensor, which was designed to monitor directly the surface charge of structurally altered maltose binding protein (MBP) upon stimulation with maltose. This study is the first report of the application of a FET biosensor to the monitoring of conformationally changed proteins. Consequently, a significant drop in current on the basis of the charge-dependent capacitance measurement has been clearly observed in response to maltose, but not for the glucose control, thereby indicating that the substrate-specific conformational properties of the target protein could be successfully monitored using the ISFET. Collectively, our results clearly suggest that ISFET provide a high fidelity system for the detection of maltose-induced structural alterations in MBP.**

© 2008 Federation of European Biochemical Societies. Published by Elsevier B.V. All rights reserved.

### 1. Introduction

Ion sensitive field effect transistor (ISFET) is a type of semiconductor biosensor, which possesses an oxide surface such as Al<sub>2</sub>O<sub>3</sub> and SiO<sub>2</sub>. ISFET technology evidences characteristics including small size, low output impedance, rapid response time, and high signal-to-noise [1,2]. All these benefits render this system a promising device, which may represent an interesting alternative to the other commonly employed electrode-type biosensors [3].

After the introduction of the ISFET biosensor by Bergveld in 1970 [4], the applications of ISFET technology have significantly expanded, and now encompass a wide-ranging field of topics. In particular, the applications of ISFET technology in biomedical science and environmental monitoring are remarkable. Thus far, a variety of ISFET-type biosensors have been developed and exploited on the basis of theoretical developments [5]. These in-

clude EnFET (Enzyme-modified FET) [6,7], ImmunoFET (Immunologically modified FET) [8,9], DNA-FET (DNA modified FET) [10,11], and CPFET (Cell-potential FET) [12,13].

The role of protein conformational changes is of critical importance in determining their functions, particularly in the case of proteins involved in cell signaling, such as enzyme activation, selective transport in channels, and other signal transduction events [14,15]. Such a relationship between structure and activity in proteins can be regulated upon binding to substrates, which depends more profoundly on the structural transitions [14]. Meanwhile, this biological mechanism based on altered protein structure in response to environmental conditions also represents an excellent mode of regulation for the detection of a variety of bioanalytes, including maltose, glucose, etc. [16,17]. The structural organization of substrates within the target protein is reflected in the properties of surface charge. Despite the importance of the conformational properties of target proteins, little study has been done regarding the detection of a structurally changed protein using electric field-based biosensors.

In this study, we utilized maltose binding protein (MBP) as a model protein for conformational change, because MBP assumes a closed conformation upon maltose binding, as demonstrated in our previous study [18]. The maltose-induced structural transition in MBP could be monitored successfully by the ISFET biosensor.

**Abbreviations:** ISFET, ion sensitive field effect transistor; MBP, maltose binding protein

\* Corresponding authors. Address: BioNanotechnology Research Center, Korea Research Institute of Bioscience and Biotechnology (KRIBB), Daejeon 305-333, South Korea. Fax: +82 42 879 8594.

E-mail addresses: [kimm@kribb.re.kr](mailto:kimm@kribb.re.kr) (M. Kim), [chungbh@kribb.re.kr](mailto:chungbh@kribb.re.kr) (B.H. Chung).

This is the first application of ISFET biosensor to the monitoring of conformational protein alterations. The ISFET biosensor might prove useful in the detection of conformationally changed proteins, thereby providing us with a new plan for a potential biosensor which can exploit charge-based capacitance measurement requiring only a minimum silicon area.

## 2. Materials and methods

### 2.1. Fabrication of ISFET device

The ISFET device was manufactured according to standard CMOS processes, as previously described [10]. This semiconductor device is comprised of a p-type (100) silicon-on-insulator (SOI) substrate as a starting material, with 150 nm thick top silicon layer and 400 nm thick buried oxide (BOX) layer. The SOI wafer has a carrier layer, which harbors an insulating intermediate layer, and the insulating intermediate layer contains an active semiconductor layer. The active region was formed via standard photolithography, followed by plasma etching to pattern the sacrificial layer. The n++ source/drain layers were then formed via phosphorous ion implantation, and the gate oxide was obtained by high-temperature dry oxidation for a field oxide growth to a thickness of 30 nm. After aluminum metallization, passivation was conducted via silicon nitride ( $\text{Si}_3\text{N}_4$ ) deposition. Finally, the gate region as a sensing layer was opened by the further etching of the  $\text{Si}_3\text{N}_4$  layer. The gate width (W) and length (L) were 200 and 10  $\mu\text{m}$ , respectively.

### 2.2. Surface modification

The ISFET surface was modified with 3-aminopropyl-tri-ethoxysilane (APTS), and followed by NHS active esterification reaction as previously described [19]. The ISFET surface was then incubated for 3 h in 50 mM nickel(II) chloride solution in order to modify the activated surface, followed by washing with DIW. The His-MBP was immobilized on the Ni(II)-coated ISFET surface. After surface modification, the homemade cell was attached to the ISFET sensing layer.

### 2.3. ISFET measurements

All measurements were conducted at room temperature (25 °C) in a homemade cell filled with 10 mM PBS buffer (pH 7.4). The threshold voltage ( $V_{\text{TH}}$ ) was determined 1.2 V from  $I_{\text{DS}}-V_{\text{GS}}$  curve as shown in Supplementary Figure (Fig. 1S).  $V_{\text{DS}}$  and  $V_{\text{GS}}$  were set to 5.0 and 2.0 V, respectively, and then the electrical measurement was carried out. The cell was then stirred gently with the PBS buffer. After the baseline stabilization of the drain current, PBS solution containing 100 mg/ml His6-MBP was added to the measurement cell, followed by a washing in fresh PBS buffer. After baseline stabilization with fresh PBS buffer, 100 mM maltose in PBS buffer was added to the MBP solution. The evaluation of the maltose-induced conformational changes was conducted via the measurement of the changes in drain current. The level of conformational changes in MBP upon maltose binding was assessed via the comparison of ISFET response without/with maltose and with glucose as a control.

### 2.4. Gene cloning, expression, and purification of MBP

The MBP gene was PCR-amplified using the 5' primer (ACT GGA TCC ATG AAA ACT GAA GAA GGT) and the 3' primer (ACT AAG CTT AGT CTG CGC GTC TTT CAG) with the *Bam*HI and *Hind*III sites, respectively. The resultant DNA fragments were then ligated with the pET 21b vector, using a ligation kit (Takara, Japan), and cloned

into the pET 21b vector using the *Bam*HI and *Hind*III sites. The plasmids were then transferred to the expression host, *E. coli* BL21 (DE3) (Stratagene, USA), and the expression and purification of His6-MBP were carried out as previously described [18].

## 3. Results and discussion

### 3.1. Rationale for ISFET-based monitoring of maltose-induced conformational changes in MBP

Proteins binding to substrate frequently induce substantial conformational alterations. A typical example of this is the maltose binding protein (MBP), which has been well characterized as a two domain hinge-bending protein (Fig. 1A). The MBP, with a molecular weight (MW) of 40 kDa, consists of 370 amino acid residues, and its dimensions are  $\sim 3 \times 4 \times 6.5$  nm [20]. As shown in Fig. 1A, MBP undergoes substantial conformational changes when maltose binds to MBP. Upon the docking of maltose with MBP, two lobes of MBP rotate  $\sim 35^\circ$ , twist laterally  $\sim 8^\circ$ , and move  $\sim 0.7$  nm closer to one another [21]. From a physicochemical viewpoint, understanding these conformational changes may provide us with important clues regarding the structural transitions associated with hinge-twist motion. In recent years, there has been an increasing interest regarding the exploitation of substrate-induced conformational changes of MBP in the field of biosensor applications [16].

In this study we reported, for the first time, a novel application of a semiconductor ISFET biosensor for the monitoring of substrate-induced conformational rearrangements in proteins. Upon maltose addition, two lobes of MBP are brought closer to each other, thereby resulting in a subsequent conformational coupling of the two domains, which is characterized by a hinge-twist motion between its two domains (Fig. 1B). As a consequence, the relative distance between MBP and the gate surface of the ISFET device are brought into spatial distance, which allows for the measurement of changes in the drain current of the ISFET biosensor (Fig. 1B), in an attempt to gain insight into the maltose-induced structural alterations in MBP.

### 3.2. ISFET surface modification

The cross-section diagram of the ISFET assembly and the ISFET measurement system are presented in Fig. 2A and B, respectively. The tested ISFET biosensor was fabricated using a standard CMOS process, as described in Section 2. First, a thin nickel film, which functioned as a matrix for His6-MBP, was formed over the ISFET gate. Prior to maltose treatment, the nickel surface was functionalized by attaching His6-MBP onto it, allowing for an excellent orientation-controlled immobilization without nonspecific binding by virtue of the specificity of affinity between histidine and the nickel film. In order to ensure the homogeneity of MBP immobilized on the ISFET surface, the MBP-modified surface was imaged via atomic force microscopy (AFM) prior to stimulation with maltose. Fig. 3A shows the AFM 3D image of immobilized-MBP (100 mg/ml) on the ISFET sensing layer, evidencing a specific binding of target proteins on the surface. The average coverage of the bare surface was set at 0% (a), and the His6-MBP on the unmodified surface was assessed as a negative control. In order to measure the relative coverage, we calculated the average surface roughness for each AFM image with provided software of the AFM (Dimension 3100; Veeco Inc.) instrument as previously reported [22]. As shown in Fig. 3A, the average coverage with the His6-MBP on the NTA-Ni(II)-coated surface ((d), 71.4%) was approximately 1.2 times higher than that obtained with NTA-Ni(II) only ((c), 59.7%), whereas the His6-MBP on the unmodified surface exhibited the absence of nonspecific binding to the ISFET surface ((b), 7.5%).

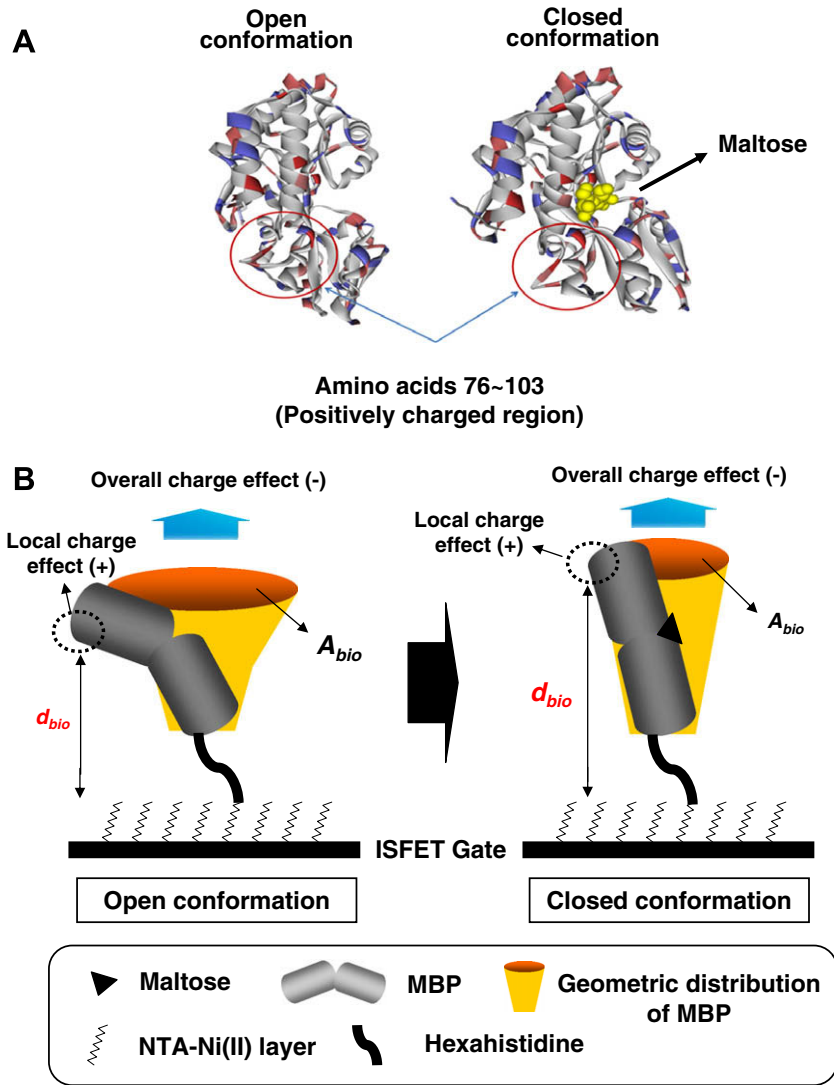


**Fig. 1.** Schematic diagram of the ISFET-based monitoring via conformational changes in MBP. (A) Structure of MBP in the open (right) and closed (left) conformations. (B) Upon binding to maltose, MBP undergoes a structural transition into closed conformations, characterized by a hinge-twist motion between its two lobes, and this is responsible for the changes in the drain current of the ISFET device.

### 3.3. Real-time monitoring of maltose-induced conformational changes in MBP using ISFET biosensor

In order to monitor the structural alterations in MBP upon stimulation with maltose, a semiconductor parameter analyzer (KEITHLEY 4200) was utilized as a measurement apparatus, as it is simple to use and allows for quick measurement. In theory, the drain current decreases in an n-type ISFET biosensor as the result of the negative charge at the gate, and the corresponding charge determines the gate potential of the ISFET device. In general, the drain current of the ISFET-type biosensor is defined as follows:

$$I_{DS} = \frac{1}{2} \mu_n C \frac{W}{L} (V_{GS} - V_{TH})^2 \quad (\text{saturation region}) \quad (1)$$

$$\frac{1}{C} = \frac{1}{C_{ox}} + \frac{1}{C_{chem}} + \frac{1}{C_{bio}} \quad (1-1)$$

$$C_{bio} = \frac{\epsilon_{bio} A}{d_{bio}} \quad (1-2)$$

where  $\mu_n$  is the electron mobility,  $C$  is total gate capacitance per unit area,  $C_{ox}$  is the gate oxide capacitance per unit area,  $C_{chem}$  is the chemical molecule capacitance per unit area,  $C_{bio}$  is the biomolecule

capacitance per unit area. Capacitance factors are connected in series.  $W$  is the gate width,  $L$  is the gate length,  $V_{TH}$  is the threshold voltage,  $\epsilon$  is the dielectric constant,  $A$  is the unit area. The factors of  $d_{bio}$  and  $V_{GS}$  are replaced by the dimensions of the macromolecules and the reference bias between the measurement solution and the biosensor, respectively. The drain current after binding MBP can be modified as follows:

$$I'_{DS} = \frac{1}{2} \mu_n C \frac{W}{L} (V_{GS} - V_{TH} + \phi_{MBP})^2 \quad (2)$$

in which  $\phi_{MBP}$  is the potential induced by the negatively charged MBP. As shown in Fig. 3B, upon the addition of MBP, the drain current of the device was reduced by approximately 2.617  $\mu A$  under a fixed output voltage of 2.0 V owing to the dominant negative charges in MBP. After the addition of maltose, the drain current can be modified as follows:

$$I''_{DS} = \frac{1}{2} \mu_n C' \frac{W}{L} (V'_{GS} - V_{TH} + \phi'_{MBP})^2 \quad (3)$$

in which  $C'$  and  $\phi'_{MBP}$  are the capacitance and the potential resulting from the conformationally altered MBP in response to maltose, respectively. When treated with maltose in the solution, the average reduction in the drain current was approximately 1.175  $\mu A$ .

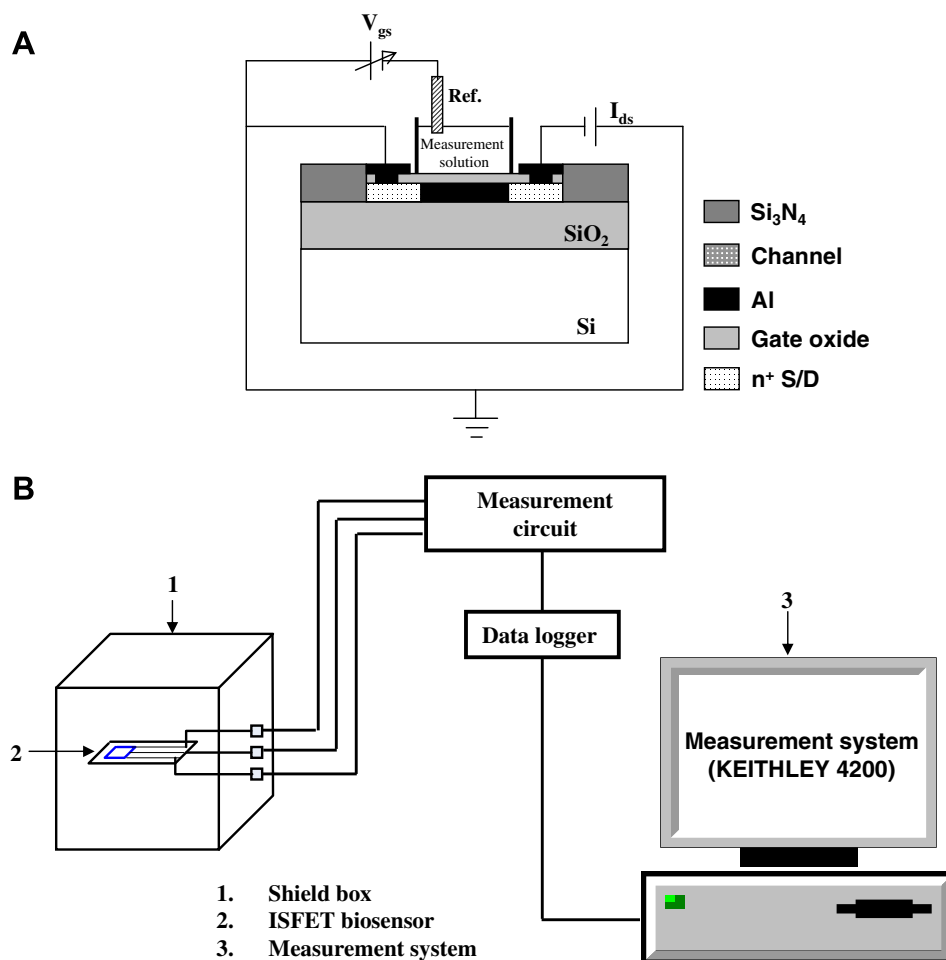


**Fig. 2.** Schematic diagram of the ISFET. (A) A cross-sectional diagram of the ISFET biosensor employed in the detection of a conformationally changed protein. (B) Diagram of the ISFET measurement system.

This considerable drop in drain current by maltose treatment can be explained by two possible directions; (1) geometric contribution, (2) charge contribution. Fig. 1B shows that MBP exhibits different geometric properties, open and closed duration distributions, as illustrated by ensemble averaged structure of protein. Maltose-free MBP in open form displays a high value of  $A_{bio}$ , whereas maltose-bound MBP in closed conformation has a relatively low  $A_{bio}$  value. Also, maltose-induced structural transitions into closed conformation increase  $d_{bio}$  between ISFET surface and MBP. Since the value of  $C_{bio}$  will be proportional to  $A_{bio}/d_{bio}$ , the value of  $C_{closed}$  is consequently smaller than  $C_{open}$  value, resulting from the reduction of  $C_{bio}$  value due to conformationally altered MBP in response to maltose. As drain current ( $I_{DS}$ ) is directly proportional to the value of  $C$  from the Eq. (1), maltose-induced conformational changes of MBP into closed conformation lead to drop in drain current, called “geometric contribution”.

The changes in drain current can be also explained in terms of “charge contribution”. MBP represents negative charge at given pH condition (pH 7.4), as its pI value is 5.07. Accordingly, immobilization of MBP onto ISFET gate surface leads to the decline of drain current. The current change can be influenced by the overall net charges in MBP. When a structural transition into the closed conformation in MBP occurred, a negatively charged MBP is supposed to contribute to the current upshift. However, this would not elucidate the response difference obtained from the present study, indicating that this may play neglectable roles, if any, in eventual change in drain current. Meanwhile, it is also worthwhile to note

that upon maltose binding, a positively charged region in MBP (amino acids 76–103) may move away from the surface, thereby resulting in the field effect performance of ISFET as a local charge effect. Based on the Eq. (1–2), the changes in current are inversely proportional to the distance  $d_{bio}$  between the sensing layer and MBP. As shown in Fig. 1B, upon maltose binding, substrate-induced MBP structural transition into closed conformation may potentially increase the relative distance between the MBP and ISFET surface, thus decreasing the drain current.

Taken together, it is thought that both “geometric effect” and “charge effect” synergistically affect the drop in drain current. In particular, the geometric characteristics associated with the geometric factors such as  $A$ ,  $d$ , and  $C$  may predominantly contribute the field effect performance of ISFET in our experimental setting. With regard to charge effect, a positively charged region of MBP (amino acids 76–103) away from the surface is thought to be responsible for the weak field force between ISFET surface and MBP.

In order to evaluate the substrate specificity, we exposed the MBP-modified ISFET surface to glucose as a negative control. As shown in Fig. 3C, no reduction in drain current was observed with MBP in response to glucose, thereby indicating the specificity of interactions occurring between MBP and maltose, and demonstrating substrate-specific conformational change. Moreover, no change in drain current was observed with maltose treatment in the absence of MBP (data not shown), excluding the possibility that the drain current of an ISFET biosensor may be influenced by the

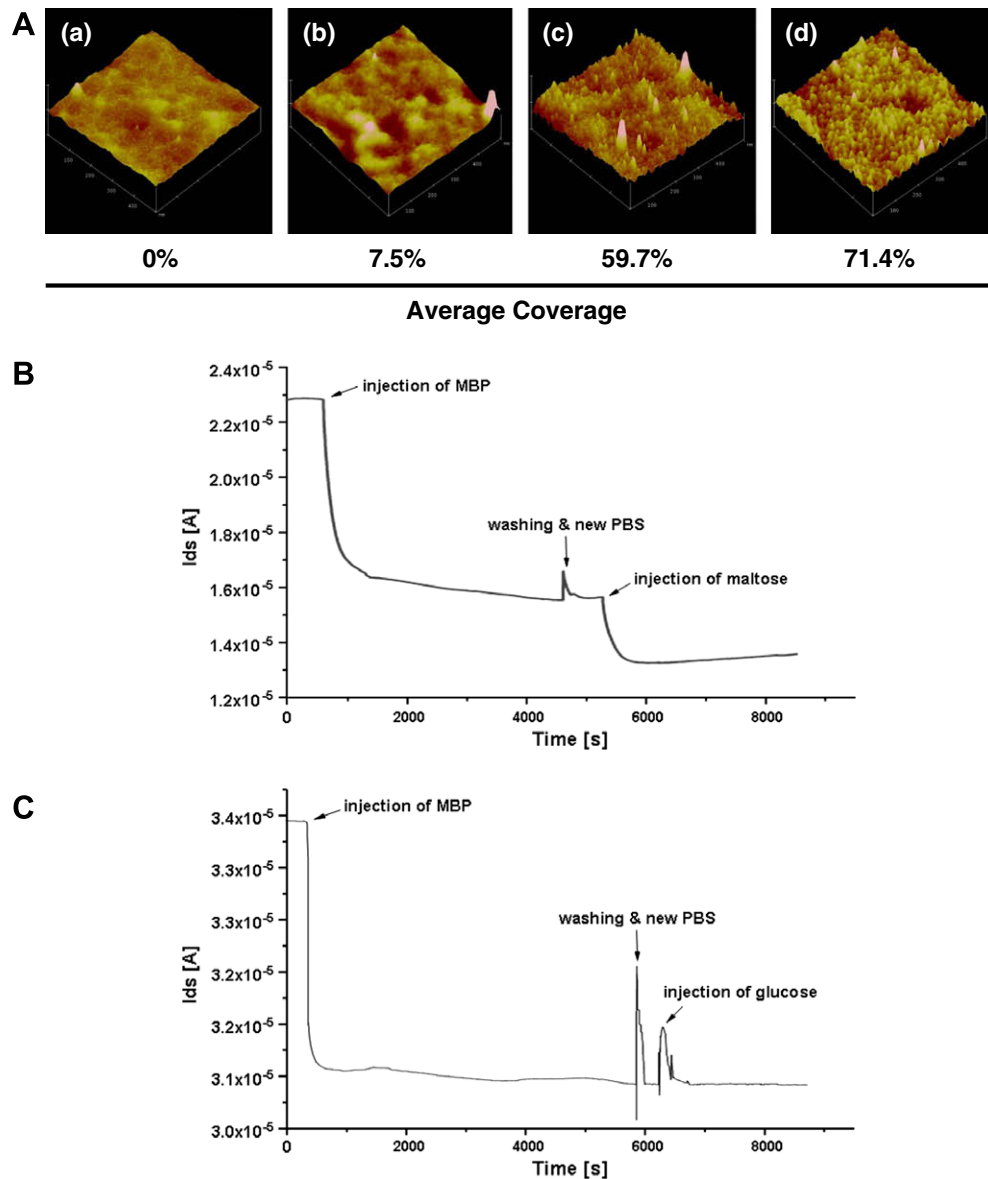


**Fig. 3.** ISFET-based monitoring of maltose-induced conformational changes in MBP. (A) AFM images of bare surface, (a) bare surface, (b) His6-MBP on unmodified surface, (c) NTA-Ni(II) surface, and (d) His6-MBP on NTA-Ni(II)-modified surface are indicated. Plot of drain current versus time after injection of maltose (100 mg/ml) (B), and glucose (100 mg/ml) (C) at 2.0 V applied voltage on the ISFET biosensor. The measurement was conducted in darkness.

substrate, thereby indicating that the ISFET data strongly reflected the fact that the open status in MBP is converted back to the closed status following maltose binding.

As well known, the electric field disappears beyond the “Debye length”, which is the distance in which mobile charge carriers screen out the external electric field. So far, this Debye length has become one of the major drawbacks in measuring the biomolecular interactions using an FET-type biosensor [5,23]. Thus, it is essentially required for the FET applications that the biomolecular reaction should occur within the Debye length. With this regard, detection of protein conformational changes like hinge-twist motions is equal to an FET-type biosensor, because structurally altered proteins in a single polypeptide can be analyzed in very close proximity to the surface, compared to protein–protein complexes, thereby enabling the sensitive detection of current changes using ISFET.

In conclusion, here we have newly applied ISFET technology to monitor conformational changes of target protein. A conforma-

tional changes of MBP, which is induced by maltose binding, was successfully assessed by an ISFET biosensor. The protein underwent the structural transition on the sensor surface upon maltose treatment, resulting in the significant reduction in the drain current of the ISFET device. Our results clearly demonstrated that the ISFET biosensor can be effectively utilized to monitor an intramolecular conformation transition.

#### Acknowledgements

This research was supported by grants from the Nano/Bio Science and Technology Program (2005-01321, MEST, Korea), and the KRIBB Initiative Research Program (KRIBB, Korea).

#### Appendix A. Supplementary data

Supplementary data associated with this article can be found, in the online version, at [doi:10.1016/j.febslet.2008.11.039](https://doi.org/10.1016/j.febslet.2008.11.039).

## References

- [1] Yuqing, M., Jianguo, G. and Jianrong, C. (2003) Ion sensitive field effect transducer-based biosensors. *Biotechnol. Adv.* 21, 527–534.
- [2] Koch, S., Woias, P., Meixner, L.K., Drost, S. and Wolf, H. (1999) Protein detection with a novel ISFET-based zeta potential analyzer. *Biosens. Bioelectron.* 14, 413–421.
- [3] Dzyadevych, S.V., Soldatkin, A.P., El'skaya, A.V., Martelet, C. and Jaffrezic-Renault, N. (2006) Enzyme biosensors based on ion-selective field-effect transistors. *Anal. Chim. Acta* 568, 248–258.
- [4] Bergveld, P. (1970) Development of an ion-sensitive solid-state device for neurophysiological measurements. *IEEE Trans. Biomed. Eng.* 17, 70–71.
- [5] Schöning, M.J. and Poghossian, A. (2002) Recent advances in biologically sensitive field-effect transistors (BioFETs). *Analyst* 127, 1137–1151.
- [6] Janata, J. and Moss, S.D. (1976) Chemically sensitive field-effect transistors. *Biomed. Eng.* 11, 241–245.
- [7] Zayats, M., Kharitonov, A.B., Katz, E., Bückmann, A.F. and Willner, I. (2000) An integrated NAD<sup>+</sup>-dependent enzyme-functionalized field-effect transistor (ENFET) system: development of a lactate biosensor. *Biosens. Bioelectron.* 15, 671–680.
- [8] Schasfoort, R.B., Kooyman, R.P., Bergveld, P. and Greve, J. (1990) A new approach to immunoFET operation. *Biosens. Bioelectron.* 5, 103–124.
- [9] Zayats, M., Raitman, O.A., Chegel, V.I., Kharitonov, A.B. and Willner, I. (2002) Probing antigen–antibody binding processes by impedance measurements on ion-sensitive field-effect transistor devices and complementary surface plasmon resonance analyses: development of cholera toxin sensors. *Anal. Chem.* 74, 4763–4773.
- [10] Kim, D.S., Jeong, Y.T., Park, H.J., Shin, J.K., Choi, P., Lee, J.H. and Lim, G. (2004) An FET-type charge sensor for highly sensitive detection of DNA sequence. *Biosens. Bioelectron.* 20, 69–74.
- [11] Fritz, J., Cooper, E.B., Gaudet, S., Sorger, P.K. and Manalis, S.R. (2002) Electronic detection of DNA by its intrinsic molecular charge. *Proc. Natl. Acad. Sci. USA* 99, 14142–14146.
- [12] Fromherz, P., Offenhäusser, A., Vetter, T. and Weis, J. (1991) A neuron-silicon junction: a Retzius cell of the leech on an insulated-gate field-effect transistor. *Science* 252, 1290–1293.
- [13] Wolf, B., Brischwein, M., Baumann, W., Ehret, R. and Kraus, M. (1998) Monitoring of cellular signalling and metabolism with modular sensor-technique: the PhysioControl-Microsystem (PCM). *Biosens. Bioelectron.* 13, 501–509.
- [14] Kim, C., Xuong, N.H. and Taylor, S.S. (2005) Crystal structure of a complex between the catalytic and regulatory (R1alpha) subunits of PKA. *Science* 307, 690–696.
- [15] Chin, D. and Means, A.R. (2000) Calmodulin: a prototypical calcium sensor. *Trends Cell Biol.* 10, 322–328.
- [16] Medintz, I.L. and Deschamps, J.R. (2006) Maltose-binding protein: a versatile platform for prototyping biosensing. *Curr. Opin. Biotechnol.* 17, 17–27.
- [17] Kamata, K., Mitsuya, M., Nishimura, T., Eiki, J. and Nagata, Y. (2004) Structural basis for allosteric regulation of the monomeric allosteric enzyme human glucokinase. *Structure* 12, 429–438.
- [18] Jeong, J., Kim, S.K., Ahn, J., Park, K., Jeong, E.J., Kim, M. and Chung, B.H. (2006) Monitoring of conformational change in maltose binding protein using split green fluorescent protein. *Biochem. Biophys. Res. Commun.* 339, 647–651.
- [19] Zourob, M., Mohr, S., Treves Brown, B.J., Fielden, P.R., McDonnell, M.B. and Goddard, N.J. (2005) An integrated metal clad leaky waveguide sensor for detection of bacteria. *Anal. Chem.* 77, 232–242.
- [20] Fehr, M., Frommer, W.B. and Lalonde, S. (2002) Visualization of maltose uptake in living yeast cells by fluorescent nanosensors. *Proc. Natl. Acad. Sci. USA* 99, 9846–9851.
- [21] Fehr, M., Ehrhardt, D.W., Lalonde, S. and Frommer, W.B. (2004) Minimally invasive dynamic imaging of ions and metabolites in living cells. *Curr. Opin. Plant Biol.* 7, 345–351.
- [22] Lee, J.M., Park, H.K., Jung, Y., Kim, J.K., Jung, S.O. and Chung, B.H. (2007) Direct immobilization of protein g variants with various numbers of cysteine residues on a gold surface. *Anal. Chem.* 79, 2680–2687.
- [23] Stern, E., Wagner, R., Sigworth, F.J., Breaker, R., Fahmy, T.M. and Reed, M.A. (2007) Importance of the Debye screening length on nanowire field effect transistor sensors. *Nano Lett.* 7, 3405–3409.